

# Memory-Critical Dynamical Buildup of Phonon-Dressed Majorana Fermion

Oliver Kästle,<sup>1,\*</sup> Ying Hu,<sup>2,3</sup> Alexander Carmele<sup>1</sup>

<sup>1</sup>*Technische Universität Berlin, Institut für Theoretische Physik,  
Nichtlineare Optik und Quantenelektronik, Hardenbergstrae 36, 10623 Berlin, Germany*

<sup>2</sup>*State Key Laboratory of Quantum Optics and Quantum Optics Devices,  
Institute of Laser Spectroscopy, Shanxi University, Taiyuan, Shanxi 030006, China*

<sup>3</sup>*Collaborative Innovation Center of Extreme Optics,  
Shanxi University, Taiyuan, Shanxi 030006, China*

(Dated: June 25, 2020)

We investigate the dynamical interplay between topological state of matter and the non-Markovian dissipation, which gives rise to a new time scale into the system dynamics due to its quantum memory. We specifically study a one-dimensional polaronic topological superconductor with phonon-dressed  $p$ -wave pairing, when a fast temperature increase in surrounding phonons induces an open-system dynamics. We show that when the memory depth increases, the Majorana edge dynamics transits from relaxing monotonically to a plateau of substantial value into a collapse-and-buildup behavior, even when the polaron Hamiltonian is close to the topological phase boundary. Above a critical memory depth, the system can approach a new dressed state of topological superconductor in equilibrium with phonons, with a nearly full buildup of the Majorana correlation asymptotically.

Exploring topological properties out of equilibrium is central in the effort to realize, probe and exploit topological states of matter in the lab [1–18]. A paradigmatic scenario is where the topological system is coupled to a Markovian bath [19–28], inducing open-dissipative dynamics that is described by a Lindblad-form master equation [29] for the time-evolved reduced system density operator. Yet, solid-state realizations of topological matter often rely on nanotechnological design strategies that restructure the environment by fine-tuning the corresponding frequency-dependent density of states. In this case, the Markovian approximation usually fails, e.g. in condensed-matter with nanostructured acoustic environments. Such non-Markovian situations can also occur when trapped ultracold atoms are immersed into superfluids. Compared to Markovian scenarios, key differences arise from the presence of quantum memory effect of non-Markovian process: the information is lost from the system to the environment but flows back at a later time. This generates a new and critical time scale into the system dynamics that is strictly absent in a Markovian context, and raises the challenge as to what are the unique dynamical consequences of the interplay between topological state of matter and the non-Markovian dissipation.

Here, we demonstrate that the quantum memory from a non-Markovian parity-preserving interaction of a topological  $p$ -wave superconductor with surrounding phonons can give rise to intriguing edge mode relaxation dynamics with no Markovian counterpart. Our study is based on the polaron master equation, describing open-dissipative dynamics of a *polaronic* topological superconductor with *phonon-renormalized* Hamiltonian parameters [see Fig. 1]. In contrast to Markovian decoherence that typically destroys topological features for long times, we show that a finite quantum memory allows for sub-

stantial preservation of topological properties away from equilibrium, even when the polaron Hamiltonian is close to the topological phase boundary [see Fig. 2 (b)]. Depending on the memory depth (i.e., the characteristic time scale of the quantum memory), the Majorana edge dynamics can monotonically relax to a plateau, or, it undergoes a collapse-and-buildup relaxation [see Fig. 2 (c)]. Remarkably, when the memory depth increases above a critical value, the Majorana correlation can nearly fully build up, corresponding to a *new polaronic state* of topological superconductor in equilibrium with phonons.

Concretely, we consider the paradigmatic Kitaev’s  $p$ -wave superconductor [30], with a superohmic coupling to a 3D structured phonon bath. The total Hamiltonian is denoted by  $H_0 = H_k + H_b$  ( $\hbar \equiv 1$ ). The Kitaev Hamiltonian  $H_k = \sum_{l=1}^{N-1} [(-Jc_l^\dagger c_{l+1} + \Delta c_l c_{l+1}) + \text{H.c.}] - \mu \sum_{l=1}^N c_l^\dagger c_l$  describes spinless fermions  $c_l, c_l^\dagger$  on a chain of  $N$  sites  $l$ , with a nearest-neighbor tunneling amplitude  $J \in \mathbb{R}$ , pairing amplitude  $\Delta \in \mathbb{R}$ , and chemical potential  $\mu$ . When  $|\mu| < 2J$  and  $\Delta \neq 0$ , the superconductor is in the topological regime featuring unpaired Majorana edge modes  $\gamma_L = \gamma_L^\dagger$  and  $\gamma_R = \gamma_R^\dagger$  at two ends [31], which exhibit a nonlocal correlation  $\theta = -i\langle \gamma_L \gamma_R \rangle = \pm 1$  that corresponds to the fermionic parity distinguishing the two degenerate ground states. The chain is coupled to a 3D structured phonon reservoir with a parity-preserving interaction, described by  $H_b = \int d^3\mathbf{k} [\omega_{\mathbf{k}} r_{\mathbf{k}}^\dagger r_{\mathbf{k}} + \sum_{l=1}^N g_{\mathbf{k}} c_l^\dagger c_l (r_{\mathbf{k}}^\dagger + r_{\mathbf{k}})]$ . Here, operator  $r_{\mathbf{k}}^{(\dagger)}$  annihilates (creates) phonons with momentum  $\mathbf{k}$  and frequencies  $\omega_{\mathbf{k}} = c_s k$ , where  $c_s$  is the sound velocity of the environment [32–40]. We choose a generic superohmic fermion-phonon coupling  $g_{\mathbf{k}}$  which features a frequency dependence modeled as a Gaussian function,  $g_{\mathbf{k}} = f_{\text{ph}} \sqrt{k/(V\sigma^2)} \exp(-k^2/\sigma^2)$  with a width  $\sigma$  and a dimensionless amplitude  $f_{\text{ph}} \ll 1$ . Such fermion-phonon interactions can represent the coupling of elec-

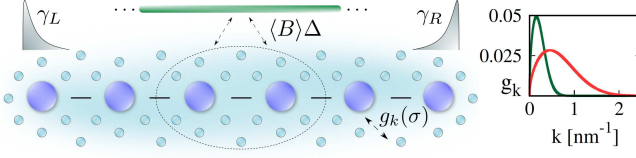


Figure 1. A polaronic Kitaev chain, with phonon-dressed spinless fermions, exhibits a renormalized  $p$ -wave pairing  $\langle B \rangle \Delta$  at temperature  $T$  [see Eq. (1)]. In the topological ground state, two unpaired Majorana edge modes  $\gamma_L, \gamma_R$  emerge. The coupling  $g_k$  to structured phonon bath features mode-dependence with a spectral width  $\sigma$ . The right panel illustrates a Gaussian profile of  $g_k$  in the momentum space (see text), respectively, for  $\sigma = 0.2$  (green) and  $\sigma = 0.6$  (red).

trons with acoustic phonons in relevant solid-state experiments and protocol proposals [41–53], and in ultra-cold atoms, can arise from coupling fermionic lattice to Bose-Einstein condensate inducing  $p$ -wave superconductivity [54–56]. We consider the topological superconductor and bath are initially in equilibrium at low temperatures, before a sudden increase in the bath temperature induces an open-system dynamics.

*Polaron master equation.* The interactions with the structured reservoir result in non-Markovian open-system dynamics, whose description - particularly on long-time scales - is a challenge due to unfavorable scaling of the Hilbert space dimension. At the heart of our following solution lies the polaron representation of the coupled system [see Fig. 1]: We derive a master equation in second-order perturbation theory of the *dressed-state* system-reservoir Hamiltonian tracing out phonons, whilst retaining the coherent process (i.e., higher order contributions) from the fermion-phonon interaction through *phonon-renormalized* Hamiltonian parameters, thus efficiently accounting for the non-Markovian and potentially strongly coupled character of the dynamics [57–69].

Defining collective bosonic operators  $R^\dagger = \int d\mathbf{k} (g_k/\omega_k) r_{\mathbf{k}}^\dagger$ , we apply a polaron transformation  $U_p = \exp[\sum_{l=1}^N c_l^\dagger c_l (R^\dagger - R)]$ , which results in  $c_l^\dagger \rightarrow e^{-(R-R^\dagger)} c_l^\dagger$  that describes phonon dressing of fermions. The transformed total Hamiltonian  $H_p \equiv U_p H_0 U_p^{-1}$  is derived as

$$H_p = \sum_{l=1}^{N-1} \left[ -J c_l^\dagger c_{l+1} + \Delta e^{-2(R-R^\dagger)} c_{l+1}^\dagger c_l^\dagger + \text{H.c.} \right] - \mu \sum_{l=1}^N c_l^\dagger c_l + \int d^3\mathbf{k} \omega_k r_{\mathbf{k}}^\dagger r_{\mathbf{k}}. \quad (1)$$

Thus the considered fermion-phonon interaction results in a polaronic Kitaev chain featuring phonon-dressed  $p$ -wave pairing, with phonon-induced quantum fluctuations. Note that the polaron transformation also renders

an energy renormalization which has been canceled by a counter term in Eq. (1) [57, 70]. This is justified given the coupled system is initially at equilibrium in present study.

Before tracing out the phononic degrees of freedom, we rewrite Eq. (1) as  $H_p = H_{p,s} + H_{p,I} + H_{p,b}$  with  $H_{p,b} = \int d\mathbf{k} \omega_k r_{\mathbf{k}}^\dagger r_{\mathbf{k}}$  for the reservoir. To recover the bare Kitaev Hamiltonian dynamics for the limiting case  $g_k \rightarrow 0$ , we introduce a Franck-Condon renormalization of  $H_{p,I}$  satisfying  $\text{Tr}_B\{[H_{p,I}, \rho(t)]\} = 0$ , with  $\rho(t)$  denoting the total density operator. The renormalized system Hamiltonian  $H_{p,s}$  is given by

$$H_{p,s} = \sum_{l=1}^{N-1} \left[ -J c_l^\dagger c_{l+1} + \Delta \langle B \rangle c_{l+1}^\dagger c_l^\dagger + \text{H.c.} \right] - \mu \sum_{l=1}^N c_l^\dagger c_l, \quad (2)$$

where the paring renormalization factor is given explicitly below. And the system-reservoir interaction in the polaron picture reads  $H_{p,I} = \Delta \sum_{l=1}^{N-1} [(e^{-2(R-R^\dagger)} - \langle B \rangle) c_{l+1}^\dagger c_l^\dagger + \text{H.c.}]$ .

Crucially, we will treat  $H_{p,I}$  in the following perturbatively in second-order Born theory, as we are interested in phonon equilibration time scales much faster than the system dynamics so that dynamical decoupling effects cannot occur [57, 62]. We then derive the polaron master equation for the reduced system density matrix  $\rho_S(t)$  of the polaron chain, obtaining (Suppl. Mat.)

$$\begin{aligned} \partial_t \rho_S(t) = & -i [H_{p,s}, \rho_S(t)] \\ & - \langle B \rangle^2 \int_0^t d\tau \left\{ (\cosh[\phi(\tau)] - 1) [X_a, X_a(-\tau) \rho_S(t)] \right. \\ & \left. - \sinh[\phi(\tau)] [X_b, X_b(-\tau) \rho_S(t)] + \text{H.c.} \right\}. \end{aligned} \quad (3)$$

Here  $X_a = -J \sum_{l=1}^{N-1} (c_l^\dagger c_{l+1}^\dagger + c_{l+1} c_l)$  and  $X_b = J \sum_{l=1}^{N-1} (c_l^\dagger c_{l+1}^\dagger - c_{l+1} c_l)$  denote collective system operators, whose dynamics obeys a *time-reversed* unitary evolution governed by the renormalized Hamiltonian  $H_{p,s}$ ,  $X_{a,b}(-\tau) \equiv e^{-iH_{p,s}\tau} X_{a,b} e^{iH_{p,s}\tau}$  (Suppl. Mat.). The  $\phi(\tau)$  represents the phonon correlation function,  $\phi(\tau) = \int d^3\mathbf{k} [2g_k(\sigma)/\omega_k]^2 \{ \coth[\hbar\omega_k/(2k_B T)] \cos(\omega_k \tau) - i \sin(\omega_k \tau) \}$ , with  $k_B$  the Boltzmann constant. The renormalization factor  $\langle B \rangle$  in Eq. (2) is determined by the initial phonon correlation,  $\langle B \rangle = \exp[-\phi(0)/2]$ , with temperature dependence.

Equation (3) provides the key equation for our study. It features a *phonon-renormalized* Hamiltonian  $H_{p,s}$  describing polarons, which exhibits temperature dependence, and a non-Markovian dissipative term in the form of a memory kernel, which involves both reservoir and system correlators  $\phi(\tau)$  and  $X_{a,b}(-\tau)$ , respectively, with a *finite memory depth* determined by the lifetime of  $\phi(\tau)$ . The memory depth critically depends on the bandwidth  $\sigma$  of fermion-phonon coupling  $g_k$  [see Fig. 2 (a)]: a larger  $\sigma$  results in a faster decay of  $\phi(t)$  and hence a smaller

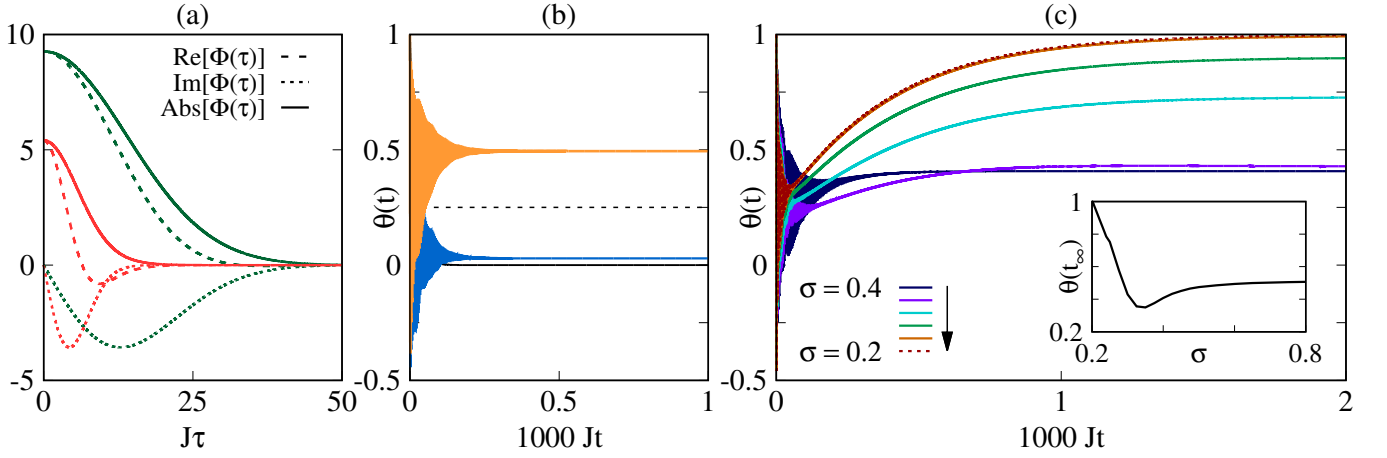


Figure 2. Non-Markovian dynamics of polaronic topological superconductor. (a) Phonon correlation function  $\phi(\tau)$  for bandwidth  $\sigma = 0.2$  (green) and  $\sigma = 0.6$  (red) of the fermion-phonon coupling  $g_k$ . (b) Comparisons of Majorana correlation  $\theta(t)$  calculated using, respectively, time-independent Lindblad-type master equation for dephasing (solid black), Eq. (3) in the Markovian limit (blue), Eq. (3) with full account of memory (orange). The dashed black line shows asymptotic  $\theta(t)$  in a coherent quench scenario  $\Delta \rightarrow \Delta\langle B \rangle$ . (c) Non-Markovian dynamics of  $\theta(t)$  for various bandwidth  $\sigma$  of phonon coupling. Corresponding steady-state value  $\theta(t_\infty)$  is shown as a function of  $\sigma$  in the inset. In all plots, the amplitude of  $g_k$  is taken as  $f_{\text{ph}} = 0.1$ , and phonon modes within  $k \in [0.0, 4.0] \text{ nm}^{-1}$  are considered. Due to the numerically very expensive size of the density matrix and its memory kernel, computations are performed for  $N = 4$  sites.

memory size, but it also leads to a smaller  $\phi(0)$  and thus a larger  $\langle B \rangle$  in both  $H_{\text{p,s}}$  and the prefactor of the memory kernel. In the limit when the system evolves much slower than the phonons, one can approximate  $X_{a,b}(-\tau) \approx X_{a,b}$ , and Eq. (3) transits into a Markovian type of master equation with a time-dependent dephasing rate  $\gamma(t)$ .

Below we investigate the Majorana edge correlation  $\theta(t) = -i\text{Tr}[\rho_s(t)\gamma_L\gamma_R]$  based on Eq. (3), starting from a factorizing system-bath state. For concreteness, we assume the system is initially at zero temperature in the ground state of a dressed Kitaev Hamiltonian with  $\Delta = J$  and  $\mu = 0$ , exhibiting even parity  $\theta(0) = 1$ . Then, a fast increase of temperature to  $T = 4\text{ K}$  results in  $\Delta \rightarrow \Delta\langle B \rangle$  of the dressed Hamiltonian, thus inducing the dynamics of polaron chain for times  $t > 0$ .

*Markovian limit.* In the Markovian limit  $X_{a,b}(-\tau) \approx X_{a,b}(0)$  of Eq. (3), the edge correlation  $\theta(t)$  rapidly decays to a very small but finite value [blue line in Fig. 2 (b)]. This is expected because dressing fermions with fast phonons induces dephasing, as has been familiar from Markovian decoherence based on time-independent Lindblad operator [see e.g., Ref. [71] and black line in Fig. 2 (b)]. Still, the non-Markovian character of the structured bath leads to a small residue correlation.

*Memory: loss vs. rephasing of topological properties.* However, the picture drastically changes when taking into account the full memory including the system's past  $X_{a,b}(-\tau)$ , as a highly non-Markovian interplay between system and reservoir unfolds. The orange line in Fig. 2 (b) shows the non-Markovian dynamics for  $\sigma = 0.6$  corresponding to  $\langle B \rangle = 0.07$ : The Majorana edge correlation

still decays (orange), in an oscillatory manner, but it relaxes to a substantial value as opposed to the Markovian limit (blue). Considering the small system size in our computation, we have verified that such asymptotic non-local correlation is genuinely of topological origin, rather than phonon-mediated long range correlations (Suppl. Mat.).

The long lived and substantial Majorana correlation in Fig. 2 (b) is quite remarkable, given that  $H_{\text{p,s}}$  is near the topological phase boundary due to a significantly suppressed renormalized pairing  $\Delta\langle B \rangle \ll \Delta$ . Indeed, without the dissipation in Eq. (3), the dynamics formally reduces to that of a coherent quench in the pairing from  $\Delta$  to  $\Delta\langle B \rangle$ . There, the Majorana correlation would approach an asymptotic value determined by the overlap of the edge mode wave functions for the pre- and post-quench topological Hamiltonians [25], which is small if the post-quench Hamiltonian is close to the phase boundary [see dashed black line in Fig. 2 (b)]. This is significantly different from the non-Markovian behavior in Fig. 2 (b) and underscores the essential role of the finite memory.

A unique feature of the memory effect is that it, because of the dependence on both  $\phi(\tau)$  and the reversed dynamics of system correlations  $X_{a,b}(-\tau)$ , *simultaneously* introduces decoherence and backflow of coherence. The dynamical consequence of this two competing processes can be intuitively understood as follows: The dressed Kitaev wire initially in its ground state is perturbed by a temperature increase to  $T$ , resulting in a renormalization of the polaron chain towards the phase boundary via  $\phi(0) =$

$\int d\mathbf{k} |2g_k(\sigma)/\omega_k|^2 \coth(\hbar\omega_k/(2k_B T))$ , which generates significant bulk excitations and populates the Majorana edge mode, changing the parity of Majorana states. Combined with phonon-assisted dephasing, this leads to strong decoherence in the polaronic Kitaev wire. On the other hand, the reversed dynamics of  $X_{a,b}(-\tau)$  acts to reinstate coherence of the  $p$ -wave pairing that is the key ingredient for topological wire. Such rephasing effect is marginal at times smaller than the characteristic time of the memory, so an irreversible loss of parity information dominates the short-time dynamics. Yet  $\phi(\tau)$  proceeds to decay over time, as its sine and cosine functions tend to cancel each other. Once  $\phi(\tau)$  approaches zero at large times, the memory reaches its full depth and the rephasing of topological properties grows due to  $X_{a,b}(-\tau)$ , giving considerable Majorana correlation in Fig. 2 (b).

*Critical memory depth.* We find the edge dynamics can exhibit distinct relaxation behavior depending crucially on the memory depth, tunable through the bandwidth  $\sigma$  of fermion-phonon coupling. Figure 2 (c) presents the non-Markovian dynamics of  $\theta(t)$  for various  $\sigma$ . Compared to  $\sigma = 0.6$  [orange line of Fig. 2 (b)], an initial decrease of  $\sigma$  results in a steeper monotonic decay of  $\theta(t)$  and a smaller asymptotic value [blue lines in Fig. 2 (c)]. However, when  $\sigma$  decreases further, the monotonic relaxation begins to transit into a non-monotonic one: While the short-time decoherence is accelerated, a buildup of edge correlation nonetheless occurs at some large times (purple line). Such buildup becomes stronger with decreased  $\sigma$ , approaching an asymptotic value larger than the  $\sigma = 0.6$  case [turquoise and green lines]. Strikingly, once  $\sigma$  surpasses a critical value, the asymptotic Majorana correlation approaches  $\theta(t_\infty) \rightarrow 1$  [orange and dotted red lines]. Figure 2 (c) summarizes the nonmonotonic variation of the asymptotic Majorana correlation  $\theta(t_\infty)$ : When  $\sigma$  decreases from a large value,  $\theta(t_\infty)$  first decreases to a minimum and then increases toward unity.

Insights into above intriguing behavior can be obtained from the fact that reducing  $\sigma$  leads to an increased memory size at the cost of a smaller  $\langle B \rangle = \exp[-\phi(0)/2]$  [see Fig. 2 (a)]; the former enhances the time scale of the time-reversed evolution of  $X_{a,b}(-\tau)$  and hence the rephasing of pairing, whereas the latter further suppresses the superconducting gap rendering  $H_{p,s}$  closer to the phase boundary as well as weakens the memory strength. When  $\sigma$  is initially decreased from 0.6, the latter effect dominates, aggravating the decay. With further reduction of  $\sigma$ , however, the former rephasing effect grows, allowing phonons and fermions to synchronize and hence backflow of parity information. Consequently, a new dressed state manages to emerge, with buildup of Majorana correlation starting to dominate over decoherence. Importantly, the existence of a critical  $\sigma$  indicates a critical memory depth, above which the system asymptotically approaches a new polaronic state of topological superconductor that is in equilibrium with phonons at  $T = 4$  K, where  $\theta \approx 1$ . The

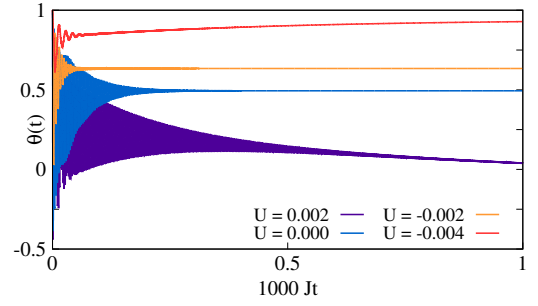


Figure 3. Non-Markovian Majorana dynamics for renormalized Hamiltonian  $H_{p,s}$  in the presence of weak  $p$ -wave interaction,  $H_{\text{int}} = U \sum_{l=1}^{N-1} (c_l^\dagger c_l - 1/2)(c_{l+1}^\dagger c_{l+1} - 1/2)$ . Other parameters, as well as initial conditions, are the same as Fig. 2.

critical value of  $\sigma$  in our case is between 0.21 and 0.20 corresponding to  $\langle B \rangle = 0.01$ , but it is model specific. We note that the fermion-phonon coupling bandwidth can be controlled, such as in solid state setups by nanotechnological design, e.g. alloys, impurities and confinement potentials [72–75].

*Concluding discussions.* The central results of our work shown in Fig. 2 are found to be robust for initially non-ideal Kitaev chains and other forms of superohmic coupling (Suppl. Mat.). Moreover, we find that the presence of a weak attractive  $p$ -wave interaction can strongly suppress the phonon-induced short-time parity loss, thus augmenting the buildup of Majorana correlation for subcritical memory depth. In Fig. 3, we calculate non-Markovian evolution of  $\theta(t)$  by including a weak  $p$ -wave interaction,  $H_{\text{int}} = U \sum_{l=1}^{N-1} (c_l^\dagger c_l - 1/2)(c_{l+1}^\dagger c_{l+1} - 1/2)$  with interaction strength  $|U| \ll 1$ , in  $H_{p,s}$  of Eq. (3) for  $\sigma = 0.6$ . Compared to the  $U = 0$  case (blue line), adding a weak attractive interaction  $U < 0$  damps out oscillations and, in particular, strongly mitigates the transient decay. Depending on  $|U|$ , the asymptotic Majorana correlation can be significantly increased (orange and red lines). An intuitive understanding can be obtained by noting that the attractive interaction is energetically favorable for coherent formation of superconducting pairing, which provides a mechanism to counteract aforementioned phonon-induced dephasing. This is consistent with the observation that for  $U > 0$ ,  $\theta(t)$  significantly declines from the  $U = 0$  case at long times (purple line), as repulsive interactions energetically suppress pairing.

Summarizing, we have demonstrated memory-critical edge dynamics in a topological superconductor with non-Markovian interaction with phonons. We show these intriguing phenomenon uniquely arises from the interplay between phonon-renormalized topological Hamiltonian and the quantum memory effect that simultaneously induces dephasing and information backflow. Our analysis is based on Kitaev chain, but we expect the essential physics to occur for a wide class of topological materials coupled to a superohmic reservoir. These discussions are



different from recent work [76–79], e.g., where the reservoir is a topological material while an impurity or a qubit coupled to it acts as a non-Markovian quantum probe. Our result is relevant to ongoing efforts aimed at realizing topological computations in experimentally realistic conditions where non-Markovian effect is inevitable. It further opens an appealing prospect as to the explorations and control of memory-dependent topological phenomena.

O.K. and A.C. gratefully acknowledge support from the Deutsche Forschungsgemeinschaft (DFG) through SFB 910 project B1 (project number 163436311). Y.H. acknowledges National Natural Science Foundation of China (Grant No. 11874038).

---

\* o.kaestle@tu-berlin.de

- [1] J. Struck, C. Ölschläger, M. Weinberg, P. Hauke, J. Simonet, A. Eckardt, M. Lewenstein, K. Sengstock, and P. Windpassinger, *Phys. Rev. Lett.* **108**, 225304 (2012).
- [2] G. Jotzu, M. Messer, R. Desbuquois, M. Lebrat, T. Uehlinger, D. Greif, and T. Esslinger, *Nature* **515**, 237 (2014).
- [3] D. Aasen, M. Hell, R. V. Mishmash, A. Higginbotham, J. Danon, M. Leijnse, T. S. Jespersen, J. A. Folk, C. M. Marcus, K. Flensberg, and J. Alicea, *Phys. Rev. X* **6**, 031016 (2016).
- [4] N. Flschner, D. Vogel, M. Tarnowski, B. S. Rem, D.-S. Lhmann, M. Heyl, J. C. Budich, L. Mathey, and K. Sengstock, *Nature Physics* **14**, 265 (2018).
- [5] W. Sun, C.-R. Yi, B.-Z. Wang, W.-W. Zhang, B. C. Sanders, X.-T. Xu, Z.-Y. Wang, J. Schmiedmayer, Y. Deng, X.-J. Liu, S. Chen, and J.-W. Pan, *Phys. Rev. Lett.* **121**, 250403 (2018).
- [6] B. Song, L. Zhang, C. He, T. F. J. Poon, E. Hagiye, S. Zhang, X.-J. Liu, and G.-B. Jo, *Science Advances* **4** (2018).
- [7] M. Tarnowski, F. N. al, N. Flschner, B. S. Rem, A. Eckardt, K. Sengstock, and C. Weitenberg, *Nature Communications* **10**, 1728 (2019).
- [8] B. Song, C. He, S. Niu, L. Zhang, Z. Ren, X.-J. Liu, and G.-B. Jo, *Nature Physics* **15**, 911 (2019).
- [9] C.-R. Yi, L. Zhang, L. Zhang, R.-H. Jiao, X.-C. Cheng, Z.-Y. Wang, X.-T. Xu, W. Sun, X.-J. Liu, S. Chen, and J.-W. Pan, *Phys. Rev. Lett.* **123**, 190603 (2019).
- [10] N. Lindner, G. Refael, and V. Galitski, *Nature Physics* **7**, 490 (2011).
- [11] M. Heyl, *Reports on Progress in Physics* **81**, 054001 (2018).
- [12] L. Zhang, L. Zhang, S. Niu, and X.-J. Liu, *Science Bulletin* **63**, 1385 (2018).
- [13] J. Alicea, *Phys. Rev. B* **81**, 125318 (2010).
- [14] Z. Shi, P. W. Brouwer, K. Flensberg, L. I. Glazman, and F. von Oppen, (2020), [arXiv:2002.01539](https://arxiv.org/abs/2002.01539).
- [15] Y. Hu, P. Zoller, and J. C. Budich, *Phys. Rev. Lett.* **117**, 126803 (2016).
- [16] J. C. Budich, Y. Hu, and P. Zoller, *Physical Review Letters* **118**, 105302 (2017).
- [17] J. W. McIver, B. Schulte, F.-U. Stein, T. Matsuyama, G. Jotzu, G. Meier, and A. Cavalleri, *Nature Physics* **16**, 38 (2020).
- [18] A. Elben, J. Yu, G. Zhu, M. Hafezi, F. Pollmann, P. Zoller, and B. Vermersch, *Science advances* **6**, 3666 (2020).
- [19] G. Goldstein and C. Chamon, *Phys. Rev. B* **84**, 205109 (2011).
- [20] S. Diehl, E. Rico, M. A. Baranov, and P. Zoller, *Nature Physics* **7**, 971 (2011).
- [21] D. Rainis and D. Loss, *Phys. Rev. B* **85**, 174533 (2012).
- [22] C.-E. Bardyn, M. A. Baranov, C. V. Kraus, E. Rico, A. İmamoğlu, P. Zoller, and S. Diehl, *New Journal of Physics* **15**, 085001 (2013).
- [23] M. J. Schmidt, D. Rainis, and D. Loss, *Phys. Rev. B* **86**, 085414 (2012).
- [24] F. L. Pedrocchi and D. P. DiVincenzo, *Phys. Rev. Lett.* **115**, 120402 (2015).
- [25] Y. Hu, Z. Cai, M. A. Baranov, and P. Zoller, *Phys. Rev. B* **92**, 165118 (2015).
- [26] F. L. Pedrocchi, N. E. Bonesteel, and D. P. DiVincenzo, *Phys. Rev. B* **92**, 115441 (2015).
- [27] H. Dehghani, T. Oka, and A. Mitra, *Phys. Rev. B* **91**, 155422 (2015).
- [28] J. C. Budich, P. Zoller, and S. Diehl, *Phys. Rev. A* **91**, 042117 (2015).
- [29] G. Lindblad, *Commun. Math. Phys.* **48**, 119 (1976).
- [30] A. Y. Kitaev, *Physics-Uspekhi* **44**, 131 (2001).
- [31] The Majorana edge modes are of the form:  $\gamma_{L/R} = \sum_j f_{L/R,j} a_j$  in the Majorana representation  $a_{2j-1} = c_j + c_j^\dagger$  and  $a_{2j} = -i(c_j - c_j^\dagger)$  of the fermionic operators, with  $f_{L/R,j}$  being exponentially localized near the left ( $L$ ) and right ( $R$ ) edges.
- [32] G. D. Mahan, *Many-particle physics* (Springer Science & Business Media, 2013).
- [33] M. Kira and S. W. Koch, *Semiconductor quantum optics* (Cambridge University Press, 2011).
- [34] V. May and O. Kühn, *Charge and energy transfer dynamics in molecular systems* (John Wiley & Sons, 2008).
- [35] M. A. Strosio and M. Dutta, *Phonons in nanostructures* (Cambridge University Press, 2001).
- [36] J. Förstner, C. Weber, J. Danckwerts, and A. Knorr, *Phys. Rev. Lett.* **91**, 127401 (2003).
- [37] B. Krummheuer, V. M. Axt, and T. Kuhn, *Physical Review B* **65**, 195313 (2002).
- [38] A. Carmele, A. Knorr, and F. Milde, *New Journal of Physics* **15**, 105024 (2013).
- [39] N. Német, S. Parkins, A. Knorr, and A. Carmele, *Phys. Rev. A* **99**, 053809 (2019).
- [40] D. Reiter, T. Kuhn, and V. M. Axt, *Advances in Physics: X* **4**, 1655478 (2019).
- [41] V. Mourik, K. Zuo, S. M. Frolov, S. R. Plissard, E. P. A. M. Bakkers, and L. P. Kouwenhoven, *Science* **336**, 1003 (2012).
- [42] Y. Oreg, G. Refael, and F. von Oppen, *Phys. Rev. Lett.* **105**, 177002 (2010).
- [43] P. W. Brouwer, M. Duckheim, A. Romito, and F. von Oppen, *Phys. Rev. Lett.* **107**, 196804 (2011).
- [44] M. T. Deng, C. L. Yu, G. Y. Huang, M. Larsson, P. Caroff, and H. Q. Xu, *Nano Letters* **12**, 6414 (2012).
- [45] L. P. Rokhinson, X. Liu, and J. K. Furdyna, *Nature Physics* **8**, 795 (2012).
- [46] A. Das, Y. Ronen, Y. Most, Y. Oreg, M. Heiblum, and H. Shtrikman, *Nature Physics* **8**, 887 (2012).
- [47] H. O. H. Churchill, V. Fatemi, K. Grove-Rasmussen,

- M. T. Deng, P. Caroff, H. Q. Xu, and C. M. Marcus, *Phys. Rev. B* **87**, 241401 (2013).
- [48] A. D. K. Finck, D. J. Van Harlingen, P. K. Mohseni, K. Jung, and X. Li, *Phys. Rev. Lett.* **110**, 126406 (2013).
- [49] S. Nadj-Perge, I. K. Drozdov, J. Li, H. Chen, S. Jeon, J. Seo, A. H. MacDonald, B. A. Bernevig, and A. Yazdani, *Science* **346**, 602 (2014).
- [50] A. Fornieri, A. M. Whiticar, F. Setiawan, E. Portols, A. C. C. Drachmann, A. Keselman, S. Gronin, C. Thomas, T. Wang, R. Kallagher, G. C. Gardner, E. Berg, M. J. Manfra, A. Stern, C. M. Marcus, and F. Nichele, *Nature* **569**, 89 (2019).
- [51] H. Ren, F. Pientka, S. Hart, A. T. Pierce, M. Kosowsky, L. Lunczer, R. Schlereth, B. Scharf, E. M. Hankiewicz, L. W. Molenkamp, B. I. Halperin, and A. Yacoby, *Nature* **569**, 93 (2019).
- [52] V. Fatemi, S. Wu, Y. Cao, L. Bretheau, Q. D. Gibson, K. Watanabe, T. Taniguchi, R. J. Cava, and P. Jarillo-Herrero, *Science* **362**, 926 (2018).
- [53] D. Larocche, D. Bouman, D. J. van Woerkom, A. Proutski, C. Murthy, D. I. Pikulin, C. Nayak, R. J. J. van Gulik, J. Nygrd, P. Krogstrup, L. P. Kouwenhoven, and A. Geresdi, *Nature Communications* **10**, 245 (2019).
- [54] L. Jiang, T. Kitagawa, J. Alicea, A. R. Akhmerov, D. Pekker, G. Refael, J. I. Cirac, E. Demler, M. D. Lukin, and P. Zoller, *Phys. Rev. Lett.* **106**, 220402 (2011).
- [55] S. Nascimbène, *Journal of Physics B: Atomic, Molecular and Optical Physics* **46**, 134005 (2013).
- [56] Y. Hu and M. A. Baranov, *Phys. Rev. A* **92**, 053615 (2015).
- [57] H. P. Breuer and F. Petruccione, *The theory of open quantum systems* (Oxford University Press, 2002).
- [58] I. Wilson-Rae and A. Imamoglu, *Phys. Rev. B* **65**, 235311 (2002).
- [59] S. Weiler, A. Ulhaq, S. M. Ulrich, D. Richter, M. Jetter, P. Michler, C. Roy, and S. Hughes, *Phys. Rev. B* **86**, 241304 (2012).
- [60] R. Manson, K. Roy-Choudhury, and S. Hughes, *Phys. Rev. B* **93**, 155423 (2016).
- [61] C. K. Lee, J. Moix, and J. Cao, *The Journal of Chemical Physics* **136**, 204120 (2012).
- [62] D. P. S. McCutcheon and A. Nazir, *New Journal of Physics* **12**, 113042 (2010).
- [63] S. Jang, Y.-C. Cheng, D. R. Reichman, and J. D. Eaves, *The Journal of Chemical Physics* **129**, 101104 (2008).
- [64] A. Kolli, A. Nazir, and A. Olaya-Castro, *The Journal of Chemical Physics* **135**, 154112 (2011).
- [65] H.-T. Chang, P.-P. Zhang, and Y.-C. Cheng, *The Journal of Chemical Physics* **139**, 224112 (2013).
- [66] A. Carmele and S. Reitzenstein, *Nanophotonics* **8**, 655 (2019).
- [67] M. Strauß, A. Carmele, J. Schleichner, M. Hohn, C. Schneider, S. Höfling, J. Wolters, and S. Reitzenstein, *Phys. Rev. Lett.* **122**, 107401 (2019).
- [68] E. V. Denning, J. Iles-Smith, and J. Mork, *Phys. Rev. B* **100**, 214306 (2019).
- [69] E. V. Denning, J. Iles-Smith, N. Gregersen, and J. Mork, *Opt. Mater. Express* **10**, 222 (2020).
- [70] A. Caldeira and A. Leggett, *Physica A: Statistical Mechanics and its Applications* **121**, 587 (1983).
- [71] A. Carmele, M. Heyl, C. Kraus, and M. Dalmonte, *Phys. Rev. B* **92**, 195107 (2015).
- [72] W. Kim, *J. Mater. Chem. C* **3**, 10336 (2015).
- [73] S. Xiong, K. Sääskilahti, Y. A. Kosevich, H. Han, D. Donadio, and S. Volz, *Phys. Rev. Lett.* **117**, 025503 (2016).
- [74] A. A. Balandin, *Journal of Nanoscience and Nanotechnology* **5**, 1015 (2005).
- [75] A. A. Balandin, E. P. Pokatilov, and D. L. Nika, *Journal of Nanoelectronics and Optoelectronics* **2**, 140 (2007).
- [76] F. Grusdt, N. Y. Yao, D. Abanin, M. Fleischhauer, and E. Demler, *Nature Communications* **7**, 11994 (2016).
- [77] A. Camacho-Guardian, N. Goldman, P. Massignan, and G. M. Bruun, *Phys. Rev. B* **99**, 081105 (2019).
- [78] G. L. Giorgi, S. Longhi, A. Cabot, and R. Zambrini, *Annalen der Physik* **531**, 1900307 (2019).
- [79] A. Ricottone, M. S. Rudner, and W. A. Coish, (2020), [arXiv:2003.00350](https://arxiv.org/abs/2003.00350).